Title

Macrophage-like nanoparticles concurrently absorbing endotoxins and proinflammatory cytokines for sepsis management

Journal

Proceedings of the National Academy of Sciences of the United States of America, 114(43)

ISSN

0027-8424

Authors

Thamphiwatana, Soracha
Angsantikul, Pavimol
Escajadillo, Tamara
et al.

Publication Date

2017-10-24

DOI

10.1073/pnas.1714267114

Peer reviewed

Macrophage-like nanoparticles concurrently absorbing endotoxins and proinflammatory cytokines for sepsis management

Soracha Thamphiwatana[a,b,1], Pavimol Angsantikul[a,b,1], Tamara Escajadillo[c,d,1], Qiangzhe Zhang[a,b], Joshua Olson[c,d], Brian T. Luk[a,b], Sophia Zhang[a,b], Ronnie H. Fang[a,b], Weiwei Gao[a,b], Victor Nizet[c,d,2], and Liangfang Zhang[a,b,2]

[a]Department of Nanoengineering, University of California, San Diego, La Jolla, CA 92093; [b]Moores Cancer Center, University of California, San Diego, La Jolla, CA 92093; [c]Department of Pediatrics, University of California, San Diego, La Jolla, CA 92093; and [d]Skaggs School of Pharmacy and Pharmaceutical Sciences, University of California, San Diego, La Jolla, CA 92093

Edited by Mark E. Davis, California Institute of Technology, Pasadena, CA, and approved September 20, 2017 (received for review August 11, 2017)

Sepsis, resulting from uncontrolled inflammatory responses to bacterial infections, continues to cause high morbidity and mortality worldwide. Currently, effective sepsis treatments are lacking in the clinic, and care remains primarily supportive. Here we report the development of macrophage biomimetic nanoparticles for the management of sepsis. The nanoparticles, made by wrapping polymeric cores with cell membrane derived from macrophages, possess an antigenic exterior the same as the source cells. By acting as macrophage decoys, these nanoparticles bind and neutralize endotoxins that would otherwise trigger immune activation. In addition, these macrophage-like nanoparticles sequester proinflammatory cytokines and inhibit their ability to potentiate the sepsis cascade. In a mouse *Escherichia coli* bacteremia model, treatment with macrophage mimicking nanoparticles, termed MΦ-NPs, reduced proinflammatory cytokine levels, inhibited bacterial dissemination, and ultimately conferred a significant survival advantage to infected mice. Employing MΦ-NPs as a biomimetic detoxification strategy shows promise for improving patient outcomes, potentially shifting the current paradigm of sepsis management.

biomimetic nanoparticle | detoxification | sepsis | lipopolysaccharide | proinflammatory cytokine

Sepsis is a life-threatening complication of bacterial infection characterized by uncontrolled systemic inflammatory response (1). Sepsis precipitates a collapse of cardiovascular function, leading to multiple organ dysfunction or failure (2, 3). Despite many efforts devoted to finding an effective treatment, the mortality rate in sepsis is very high, and the number of hospitalizations resulting from the condition continues to rise (4, 5). Endotoxin, an important pathogenic trigger of Gram-negative bacterial sepsis, induces a systemic inflammatory response characterized by production of proinflammatory cytokines and nitric oxide, fever, hypotension, and intravascular coagulation, culminating in septic shock (6). Emerging evidence suggests that the systemic spread of endotoxin from sites of infection, rather than bacteremia itself, is crucial in the pathogenesis of this dramatic immune dysregulation (7, 8). Since higher levels of endotoxin correlate to worsened clinical outcomes (9, 10), effective endotoxin removal is a critical component of successful sepsis management.

Endotoxin neutralization and elimination present various challenges. While all endotoxins share a common architecture, they vary greatly in their structural motifs across bacterial genus, species, and strain (11, 12). Accordingly, endotoxin interactions with ligands can differ substantially, which poses challenges for structure-based neutralization strategies. Antibiotics effective in neutralizing endotoxin such as polymyxins have limits on their clinical utility due to their strong nephrotoxicity and neurotoxicity (13, 14). Attaching these molecules to solid-phase carriers for hemoperfusion can retain their endotoxin-binding properties while minimizing the toxic effects, but clinical evidence of therapeutic efficacy has yet to be established (15, 16). In addition, such solid-phase perfusion strategies are impractical in resource-limited environments (17).

Recently, cell membrane-coated nanoparticles have emerged as a biomimetic nanomedicine platform, enabling a broad range of biodetoxification applications (18, 19). In particular, nanoparticles coated with membranes derived from red blood cells (denoted RBC nanosponges) have taken advantage of functional similarities shared by various bacterial pore-forming toxins to neutralize their cytolytic activity regardless of molecular structure (20, 21). These unique core-shell nanoparticles exhibit prolonged systemic circulation, preventing further bioactivity of the absorbed toxins and diverting them away from their intended cellular targets. RBC nanosponges have also been developed as therapeutic detoxification agents to neutralize pathological antibodies in autoimmune diseases (22) and organophosphate nerve agents (23).

The therapeutic potential of membrane-coated nanoparticles for broad-spectrum detoxification inspired us to develop biomimetic nanoparticles for endotoxin removal, potentially enabling effective sepsis management. In sepsis, endotoxin, also referred to as lipopolysaccharide (LPS), is released from the bacteria during cell division, cell death, or under antibiotic treatment, whereupon it is recognized as a pathogen-associated molecular pattern (PAMP) by sentinel immune cells, including monocytes and macrophages

Significance

Clinical evidence has indicated that the systemic spread of endotoxins from septic infection plays a crucial role in the pathogenesis of Gram-negative bacterial sepsis. However, currently there are no effective ways to manage the diverse endotoxins released by different bacterial genus, species, and strain. Herein, we demonstrate the therapeutic potential of a macrophage-like nanoparticle for sepsis control through a powerful two-step neutralization process: endotoxin neutralization in the first step followed by cytokine sequestration in the second step. The biomimetic nanoparticles possess an antigenic exterior identical to macrophage cells, thus inheriting their capability to bind to endotoxins and proinflammatory cytokines. This detoxification strategy may provide a first-in-class treatment option for sepsis and ultimately improve the clinical outcome of patients.

Author contributions: S.T., P.A., T.E., R.H.F., W.G., V.N., and L.Z. designed research; S.T., P.A., T.E., Q.Z., J.O., B.T.L., S.Z., R.H.F., and W.G. performed research; S.T., P.A., T.E., Q.Z., J.O., B.T.L., S.Z., R.H.F., W.G., V.N., and L.Z. analyzed data; and S.T., P.A., T.E., R.H.F., W.G., V.N., and L.Z. wrote the paper.

The authors declare no conflict of interest.

This article is a PNAS Direct Submission.

[1]S.T., P.A., and T.E. contributed equally to this work.

[2]To whom correspondence may be addressed. Email: vnizet@ucsd.edu or zhang@ucsd.edu.

(24, 25). In the bloodstream, LPS-binding protein (LBP) binds with high affinity to LPS via lipid A, and the LPS–LBP complex subsequently engages the pattern recognition receptor (PRR) CD14 present on the macrophage cell surface (26, 27). Following this binding interaction, LPS can induce various changes in immune cell activity. For example, LPS induces a dose-dependent production of nitric oxide (NO), which can be cytotoxic at high levels (10). LPS binding to macrophages also activates the PRR Toll-like receptor 4 (TLR4), which plays a significant role in the regulation of bacterial phagocytic uptake (28), intracellular trafficking, and macrophage cell death (29, 30). Furthermore, LPS-induced engagement of TLR4 activates the nuclear factor-κB (NF-κB) transcription factor, resulting in the production and release of potent proinflammatory cytokines, such as tumor necrosis factor (TNF), interleukin 6 (IL-6), and IFN-γ (31, 32).

Compelled by the critical roles played by macrophages and their PRR in endotoxin signaling, here we develop biomimetic nanoparticles consisting of a biodegradable polymeric nanoparticle core coated with cell membrane derived from macrophages (denoted MΦ-NPs, Fig. 1*A*). MΦ-NPs possess an antigenic exterior identical to the source macrophage cells, thus inheriting their capability to bind to endotoxins. In addition, MΦ-NPs act as decoys to bind to cytokines, inhibiting their ability to potentiate downstream inflammation cascades, i.e., pathological "cytokine storm." These two functionalities together enable effective intervention during uncontrolled immune activation, providing a therapeutic intervention with significant potential for the management of sepsis.

Results and Discussion

The preparation of MΦ-NPs was divided into two steps. In the first step, cell membranes from J774 mouse macrophages were derived and purified using a process involving hypotonic lysis, mechanical disruption, and differential centrifugation. In the second step, we used a sonication method to form membrane vesicles and subsequently fused them onto poly(lactic-*co*-glycolic acid) (PLGA) cores to create MΦ-NPs. Following membrane fusion, the diameter of the nanoparticles measured with dynamic light scattering (DLS) increased from 84.5 ± 1.9 nm to 102.0 ± 1.5 nm, corresponding to the addition of a bilayered cell membrane onto the polymeric cores (Fig. 1*B*). Meanwhile, the surface zeta potential changed from −41.3 ± 3.6 mV to −26.7 ± 3.1 mV, likely due to charge screening by the membrane. The engineered MΦ-NPs were stained with uranyl acetate and visualized with transmission electron microscopy (TEM), revealing a spherical core-shell structure, in which the PLGA core was wrapped with a thin shell (Fig. 1*C*). Following their formulation, MΦ-NPs were suspended in 1× PBS and 50% serum, respectively, and demonstrated excellent stability in size and membrane coating over 72 h, as monitored by DLS (Fig. 1*D*). Improved colloidal stability is attributable to the stabilizing effect of hydrophilic surface glycans on the macrophage membrane. Together, these results demonstrate the successful coating of PLGA cores with unilamellar macrophage membranes.

Through membrane coating, MΦ-NPs inherit key biological characteristics of the source cells. By Western blot analysis, we verified that MΦ-NPs maintained critical membrane proteins responsible for LPS binding, including CD14 and TLR4 (Fig. 1*E*). Representative cytokine-binding receptors were also preserved, including CD126 and CD130 for IL-6, CD120a, and CD120b for TNF, and CD119 for IFN-γ. Indeed, the membrane derivation process resulted in significant protein enrichment for these molecules. Following i.v. administration, the systemic circulation time of MΦ-NPs was measured by labeling the nanoparticles with a hydrophobic DiD fluorophore (Fig. 1*F*). At 24 h and 48 h, respectively, MΦ-NPs showed 29% and 16% retention in the blood. Based on a two-compartment model applied in previous studies to fit nanoparticle circulation results, the elimination half-life was calculated as 17.2 h (33, 34). To further evaluate their potential for systemic applications, we investigated

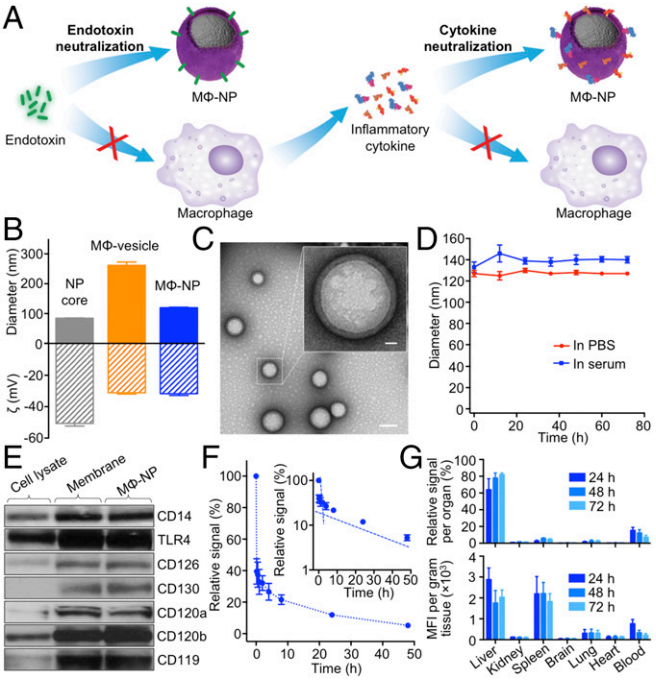

Fig. 1. Formulation and characterization of macrophage membrane-coated nanoparticles (MΦ-NPs). (*A*) Schematic representation of using MΦ-NPs to neutralize endotoxins and proinflammatory cytokines as a two-step process for sepsis management. (*B*) Hydrodynamic size (diameter, nanometers) and surface zeta potential (ζ, millivolts) of PLGA polymeric cores before and after coating with macrophage membrane as measured by dynamic light scattering ($n = 6$). (*C*) TEM images of MΦ-NPs negatively stained with uranyl acetate. (Scale bar: 100 nm.) (*Inset*) The roomed-in view of a single MΦ-NP. (Scale bar: 10 nm.) (*D*) Stability of MΦ-NPs in 1× PBS or 50% FBS, determined by monitoring particle size (diameter, nanometers), over a span of 72 h. (*E*) Representative protein bands of macrophage cell lysate, membrane vesicles, and MΦ-NPs resolved using Western blotting. (*F*) DiD-labeled MΦ-NPs were injected i.v. via the tail vein of mice. At various time points, blood was collected and measured for fluorescence (excitation/emission = 644/670 nm) to evaluate the systemic circulation lifetime of the nanoparticles ($n = 6$). (*Inset*) The semilog plot of fluorescence signal at various time points. (*G*) Biodistribution of the MΦ-NPs collected by injecting DiD-labeled MΦ-NPs i.v. into the mice. At each time point (24, 48, and 72 h), the organs from a randomly grouped subset of mice were collected, homogenized, and quantified for fluorescence. Fluorescence intensity per gram of tissue and relative signal per organ were compared ($n = 6$).

the in vivo tissue distribution of the MΦ-NPs (Fig. 1*G*). When analyzed per organ, MΦ-NPs were distributed mainly in the blood and the liver. Per gram of tissue, MΦ-NPs were principally contained in the liver and spleen, two primary organs of the reticuloendothelial system (RES). Meanwhile, significant fluorescence was also observed in the blood. As the blood fluorescence decreased, a corresponding increase in signal was observed in the liver, suggesting the uptake of MΦ-NPs by the RES over time.

We next examined the ability of MΦ-NPs to bind to LPS, which is known to first form high-affinity complexes with LBP. These complexes then bind to TLR4 through CD14, which are both present on the cell surface of macrophages. To test the effect of LBP on LPS binding to MΦ-NPs, we mixed the nanoparticles with FITC-LPS conjugate, incubated the mixture at 37 °C, then collected the MΦ-NPs by ultracentrifugation to compare their FITC fluorescence intensity to that of the supernatant. As shown in Fig. 2*A*, in the absence of LBP, nearly 80% of LPS remained in the solution. However, with addition of LBP, 90% of LPS was pelleted into the supernatant, indicating a significant increase in binding to MΦ-NPs. Meanwhile, when MΦ ghost instead of MΦ-NPs was

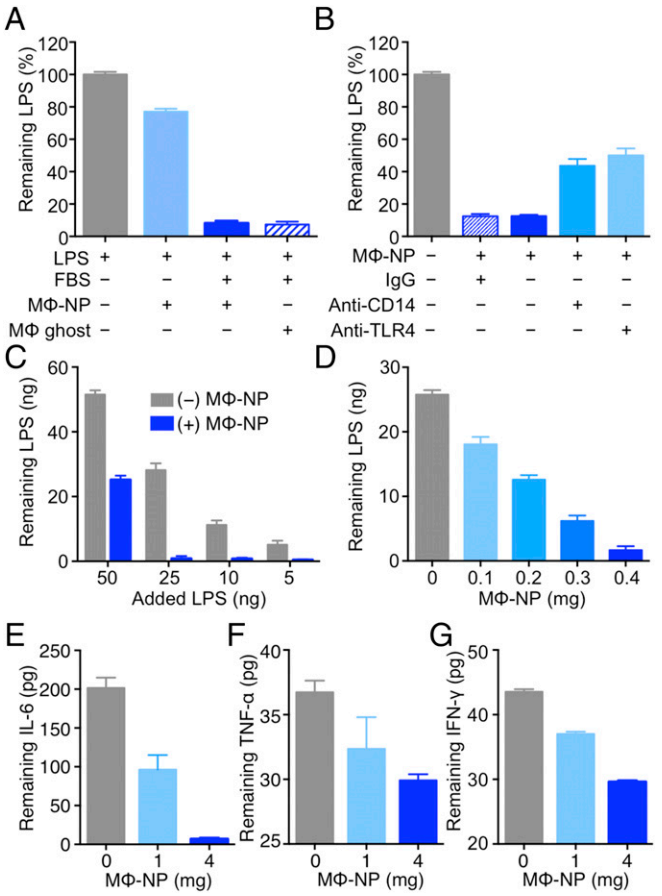

Fig. 2. In vitro LPS and proinflammatory cytokine removal with MΦ-NPs. (*A*) LPS removal with MΦ-NPs with and without LPS binding protein (LBP) supplemented from FBS. MΦ ghost with an equivalent amount of protein was included as a control to assess membrane activity loss. (*B*) LPS removal with MΦ-NPs with and without nonspecific IgG and antibodies blocking CD14 and TLR4, respectively. (*C*) Quantification of LPS removal with a fixed amount of MΦ-NPs (0.4 mg) while varying the amount of added LPS. (*D*) Quantification of LPS removal with a fixed amount of LPS (25 ng) while varying the amount of added MΦ-NPs. (*E*–*G*) Removal of proinflammatory cytokines, including (*E*) IL-6, (*F*) TNF-α, and (*G*) IFN-γ, with MΦ-NPs. In all studies, three samples were used in each group.

used (equivalent protein amount), the reduction of LPS was comparable, indicating the preservation of membrane activity during nanoparticle formulation. In addition, while nonspecific IgG from human serum showed no effect to LPS binding, the amount of unbound LPS remaining in the supernatant increased upon addition of anti-CD14 or anti-TLR4 antibodies, indicating that both macrophage PRRs mediated binding interactions between LPS and MΦ-NPs (Fig. 2*B*). Overall, compared with macrophages, MΦ-NPs showed similar dependence on LBP, TLR4, and CD14 in binding with LPS, suggesting that MΦ-NPs inherit the biological characteristics of the source cells.

Next, we quantified the LPS removal capacity of MΦ-NPs through two sets of experiments. First, we fixed the quantity of MΦ-NPs at 0.4 mg and incubated them with varying amounts of LPS (5, 10, 25, and 50 ng, respectively). After collecting nanoparticles with ultracentrifuge, it was found that 0.4 mg MΦ-NPs neutralized up to 25 ng LPS (Fig. 2*C*). In the second experiment, we fixed the total amount of LPS at 25 ng and varied the amounts of MΦ-NPs (0, 0.1, 0.2, 0.3, and 0.4 mg, respectively). When the MΦ-NP concentration was increased from 0.1 to 0.4 mg, a linear decrease of LPS remaining in the supernatant was observed, with 0.4 mg MΦ-NPs again required to neutralize 25 ng LPS (Fig. 2*D*). Together, the dual assays indicate a removal capacity of 62.5 ng LPS per milligram of MΦ-NPs.

The ability of MΦ-NPs to sequester proinflammatory cytokines, including IL-6, TNF, and IFN-γ, was also investigated. Solutions with known initial concentrations of the cytokines were added to different concentrations of MΦ-NPs and incubated at 37 °C for 30 min, at which time nanoparticles were removed by ultracentrifugation and the amount of cytokine remaining in the supernatant was quantified. As shown in Fig. 2 *E*–*G*, 1 mg of MΦ-NPs removed 105.1 pg of IL-6, 4.3 pg of TNF, and 6.5 pg of IFN-γ from the mixture, corresponding to cytokine removal efficiencies of 52.6%, 11.6%, and 14.8%, respectively. When 4 mg of MΦ-NPs was added, 194.4 pg of IL-6, 6.7 pg of TNF, and 13.9 pg of IFN-γ were removed from the mixture, corresponding to cytokine removal yields of 97.2%, 18.1%, and 31.6%, respectively. Thus, MΦ-NPs can effectively sequester various types of proinflammatory cytokines in a concentration-dependent manner.

To evaluate functional neutralization of LPS, we used engineered HEK293 TLR4 reporter cells that produce secreted embryonic alkaline phosphatase (SEAP) in response to TLR4 activation (Fig. 3*A*). When free LPS was added into the cell culture, pronounced TLR4 activation was observed within 5 h. However, when LPS was incubated with MΦ-NPs before their addition to the culture, TLR4 activation was abrogated. Incubation of LPS with RBC-NPs and PLGA nanoparticles functionalized with synthetic polyethylene glycol (PEG-NPs) were ineffective in inhibiting TLR4 activation, confirming that LPS neutralization was specific to MΦ-NPs. LPS induces macrophage overproduction of intracellular nitric oxide (iNO) by inducible NO synthase (10), which triggers further inflammatory cascades in activated cells. Macrophages incubated

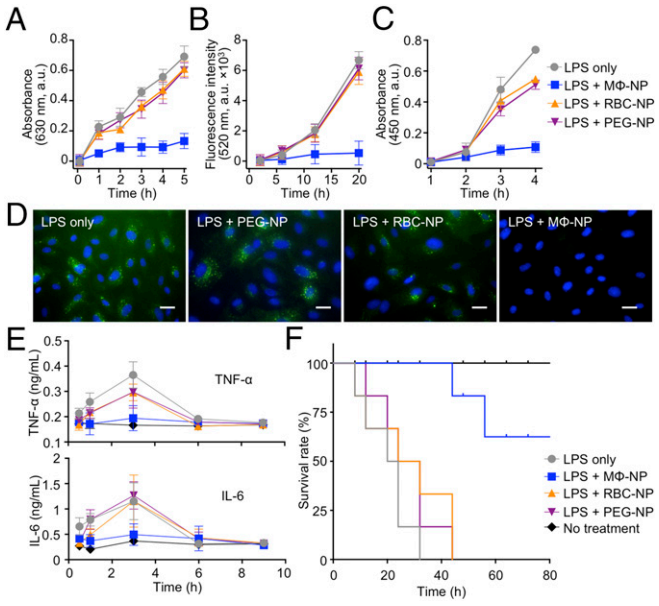

Fig. 3. In vitro and in vivo LPS neutralization with MΦ-NPs. (*A*–*C*) LPS-inducible cell functions, including (*A*) TLR4 activation on HEK293 cells, (*B*) intracellular nitric oxide (iNO) production from J774 macrophages, and (*C*) E-selectin expression of HUVECs, were studied by stimulating corresponding cells with LPS alone or LPS mixed with MΦ-NPs, RBC-NPs, or PEG-NPs, respectively. (*D*) Fluorescent images collected from samples in *C* after 4 h of incubation. Cells were stained with mouse anti-human E-selectin, followed by staining with anti-mouse IgG Alexa 488 conjugates (green) and DAPI (blue). (Scale bars: 5 μm.) Three samples were used in each group. (*E* and *F*) For in vivo evaluation, (*E*) levels of proinflammatory cytokines, including TNF-α and IL-6, in plasma ($n = 6$) and (*F*) survival ($n = 10$) were studied after injecting mice with LPS alone or LPS mixed with MΦ-NPs, RBC-NPs, or PEG-NPs. Untreated mice were also included as a control group.

with free LPS showed a continual increase of iNO, whereas LPS incubated with MΦ-NPs was unable to enhance iNO production, revealing a clear inhibitory effect (Fig. 3*B*); control RBC-NPs or PEG-NPs had no such activity.

Endothelial cells respond to minute LPS exposures by rapidly inducing expression of the cell adhesion molecule E-selectin (35). We incubated cultured human umbilical vein endothelial cells (HUVECs) with LPS and quantified E-selectin expression by enzyme immunoassay. As shown in Fig. 3*C*, 10 ng/mL LPS caused a continuous increase in HUVEC E-selectin expression; but this increase was completely blocked by coincubation with 1 mg/mL of MΦ-NPs. Control RBC-NPs and PEG-NPs did not inhibit the overexpression of E-selectin by HUVECs, confirming the specificity of MΦ-NPs in LPS neutralization. Three hours after adding LPS, cells were also stained with antibodies to fluorescently label E-selectin. Under the microscope, HUVECs incubated with LPS alone, LPS with RBC-NPs, and LPS with PEG-NPs, showed strong labeling in the cytoplasmic and nuclear peripheral regions with a fluorescent anti–E-selectin antibody; in contrast, little expression was observed on HUVECs incubated with LPS together with MΦ-NPs (Fig. 3*D*). These results further confirm the capability of MΦ-NPs to functionally neutralize LPS.

LPS neutralization by MΦ-NPs in vivo was evaluated in mice by examining inhibition of acute inflammatory responses to endotoxin. LPS (5 μg/kg) was injected via tail vein and blood collected at various time points to measure the level of proinflammatory cytokines, including TNF and IL-6 by ELISA. Cytokine levels reached maximums 3 h following injection of LPS alone, returning to baseline levels by 6 h. In the treatment group where MΦ-NPs at a dosage of 80 mg/kg were injected immediately after LPS, no increase in cytokine levels was observed. In contrast, when MΦ-NP treatment was replaced with RBC-NPs or PEG-NPs, cytokine levels followed similar kinetics to the LPS-only group. These studies demonstrate potent and specific LPS neutralization by the MΦ-NPs in vivo.

To further validate the in vivo LPS neutralization capability of MΦ-NPs, we sensitized mice to lethal effects of LPS using 800 mg/kg D-galactosamine hydrochloride (36), 30 min before LPS ± nanoparticle injection. A single dose of LPS (5 μg/kg) caused 100% mortality in the D-galactosamine-sensitized mice within 32 h of injection. Mice in the treatment groups ($n = 10$) received an i.v. injection of MΦ-NPs, RBC-NPs, or PEG-NPs at a dose of 200 mg/kg. In the group treated with MΦ-NPs, 60% of mice survived the lethal LPS challenge, whereas RBC-NPs and PEG-NPs failed to significantly improve survival rate in the LPS-challenged mice. These results together validate the potential of MΦ-NPs as endotoxin bioscavengers.

Finally, the therapeutic potential of MΦ-NPs was examined in a live infection model of Gram-negative bacterial sepsis. Mice were challenged intraperitoneally with a lethal dose of *Escherichia coli* (1×10^7 cfu) and treated with either MΦ-NPs (300 mg/kg) or 10% sucrose solution as the vehicle control 30 min after bacterial challenge. In this lethal challenge model, all animals in the control group treated with sucrose solution died, whereas 4 of 10 animals treated with a single dose of MΦ-NPs reached the experimental endpoint of 60 h, revealing a significant survival benefit ($P < 0.05$, Fig. 4*A*). In another cohort of mice, we examined acute bacterial dissemination to key organs, including the blood, spleen, kidney, and liver, 4 h after bacterial challenge ± MΦ-NP treatment. In the blood and spleen of the mice treated with MΦ-NPs, bacterial counts were significantly lower compared with those of the control group, whereas the kidney and liver from mice of both groups showed comparable bacterial counts (Fig. 4*B*). Reduction of bacterial burden in the blood and spleen conferred by MΦ-NPs corresponded to a significant reduction of proinflammatory cytokines, including IL-6, TNF-α, and IFN-γ, in these organs (Fig. 4*C*). Reversal of the pathologic processes of septicemia and cytokine storm to favor improved bactericidal clearance is certainly multifactorial, but may include reduced development of macrophage LPS tolerance by its sequestration, competitive inhibition of immunosuppressive cytokines such as IL-10, and absorption of bacterial cytotoxins (e.g., *E. coli* pore-forming α-hemolysin) or immunosuppressive factors [e.g., *E. coli* TIR-containing protein C (TcpC)].

In summary, we have demonstrated a therapeutic potential of MΦ-NPs for sepsis control through an apparent two-step neutralization process: LPS neutralization in the first step followed by cytokine sequestration in the second step. MΦ-NPs function as an LPS and cytokine decoy, binding the proinflammatory factors through their cognate PRR and cytokine receptors in a manner decoupled from signal transduction and transcriptional activation of macrophage inflammatory cascades. By thus inhibiting the systemic inflammatory response, MΦ-NPs confer a significant survival benefit during septic shock. Unlike conventional endotoxin neutralization agents that compete with endotoxin binding pathways and may be associated with significant clinical toxicity, MΦ-NPs take advantage of the common functionality of endotoxin binding to macrophages, allowing for a "universal" neutralization approach across different Gram-negative bacterial genus, species, and strains. The top-down fabrication of MΦ-NPs effectively replicates endotoxin-binding motifs on the target cells that are otherwise difficult to identify, purify, and conjugate. Coating macrophage membranes onto nanoparticle surfaces significantly increases the surface-to-volume ratio of given membrane materials, which is critical for efficient endotoxin neutralization.

In theory, similar first-step benefits as an adjunctive therapeutic agent could be afforded by MΦ-NPs against Gram-positive bacterial sepsis pathogens, by scavenging lipoteichoic acids and

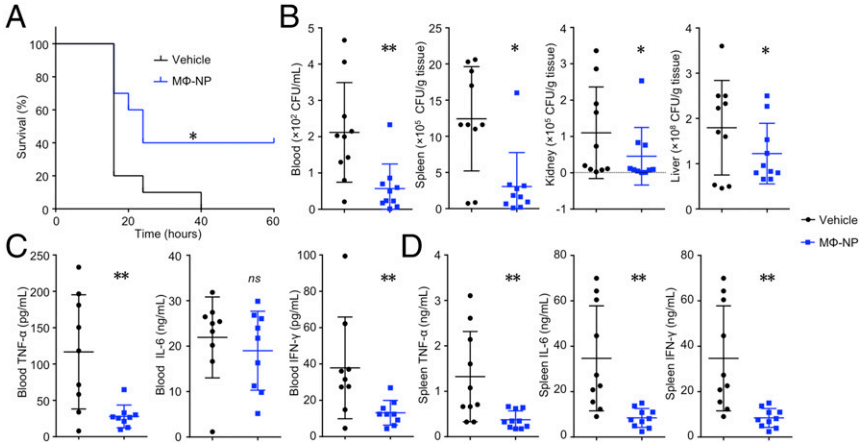

Fig. 4. In vivo therapeutic efficacy of MΦ-NPs evaluated with a mouse bacteremia model. (*A*) Survival curve of mice with bacteremia after treatment with MΦ-NPs ($n = 10$). (*B*) Bacteria enumeration in blood, spleen, kidney, and liver at 4 h after MΦ-NPs were intraperitoneally injected. (*C* and *D*) Proinflammatory cytokines, including IL-6, TNF-α, and IFN-γ, from the blood and spleen were quantified with a cytometric bead array (ns, not significant; $*P < 0.05$, $**P < 0.01$).

peptidoglycan via cognate PRRs TLR2/6, or fungal sepsis pathogens, by scavenging cell wall β-glucans with cognate PRR Dectin-1; although these indications remain to be studied in the manner undertaken with LPS/*E. coli* in the current paper. Moreover, in septic shock caused by any pathogen, second-step cytokine sequestration properties could be seen to mitigate the pathologic damage of cytokine storm. Given a likely i.v. route of administration, however, the pharmacodynamics efficacy of MΦ-NPs against tissue foci of infection such as pneumonia, peritonitis, or bone/soft tissue infections would have to be validated. Meanwhile, novel LPS-binding ligands have been engineered and applied for endotoxin neutralization and detoxification in sepsis (37). With a lipid-like structure, they can be introduced onto MΦ-NPs through methods such as lipid insertion (38) or membrane hybridization (39), both of which have been validated for functionalizing nanoparticles coated with different cell membranes. Overall, MΦ-NPs represent a promising biomimetic detoxification strategy that may ultimately improve the clinical outcome of sepsis patients, potentially shifting the current paradigm of clinical detoxification therapy.

Materials and Methods

Macrophage Membrane Derivation. The murine J774 cell line was purchased from the American Type Culture Collection (ATCC) and maintained in Dulbecco's modified Eagle medium (DMEM) (Invitrogen) supplemented with 10% FBS (HyClone) and 1% penicillin–streptomycin (pen–strep) (Invitrogen). Plasma membrane was collected according to a previously published centrifugation method (40). Specifically, cells were grown in T-175 culture flasks to full confluency and detached with 2 mM EDTA (USB Corporation) in PBS (Invitrogen). The cells were washed with PBS three times (500 × *g* for 10 min each) and the cell pellet was suspended in homogenization buffer containing 75 mM sucrose, 20 mM Tris·HCl (pH = 7.5, MediaTech), 2 mM $MgCl_2$ (Sigma-Aldrich), 10 mM KCl (Sigma-Aldrich), and one tablet of protease/phosphatase inhibitors (Pierce, Thermo Fisher Scientific). The suspension was loaded into a Dounce homogenizer and the cells were disrupted with 20 passes. Then the suspension was spun down at 3,200 × *g* for 5 min to remove large debris. The supernatant was collected and centrifuged at 20,000 × *g* for 25 min, after which the pellet was discarded and the supernatant was centrifuged at 100,000 × *g* for 35 min. After the centrifugation, the supernatant was discarded and the plasma membrane was collected as an off-white pellet for subsequent experiments. Membrane protein content was quantified with a Pierce BCA assay (Life Technologies).

MΦ-NP Preparation and Characterization. MΦ-NPs were formulated in two steps. In the first step, ∼80-nm polymeric cores were prepared using 0.67 dL/g carboxyl-terminated 50:50 PLGA (LACTEL absorbable polymers) through a nanoprecipitation method. The PLGA polymer was first dissolved in acetone at a concentration of 10 mg/mL. Then 1 mL of the solution was added rapidly to 3 mL of water. For fluorescently labeled PLGA cores, 1,1′-dioctadecyl-3,3,3′,3′-tetramethylindodicarbocyanine perchlorate (DiD, excitation/emission = 644 nm/665 nm; Life Technologies) was loaded into the polymeric cores at 0.1 wt%. The nanoparticle solution was then stirred in open air for 4 h to remove the organic solvent. In the second step, the collected macrophage membranes were mixed with nanoparticle cores at a membrane protein-to-polymer weight ratio of 1:1. The mixture was sonicated with a Fisher Scientific FS30D bath sonicator at a frequency of 42 kHz and a power of 100 W for 2 min. Nanoparticles were measured for size and size distribution with DLS (ZEN 3600 Zetasizer, Malvern). All measurements were done in triplicate at room temperature. Serum and PBS stabilities were examined by mixing 1 mg/mL of MΦ-NPs in water with 100% FBS and 2× PBS, respectively, at a 1:1 volume ratio. Membrane coating was confirmed with transmission electron microscopy (TEM). Briefly, 3 μL of nanoparticle suspension (1 mg/mL) was deposited onto a glow-discharged carbon-coated copper grid. Five minutes after the sample was deposited, the grid was rinsed with 10 drops of distilled water, followed by staining with a drop of 1 wt% uranyl acetate. The grid was subsequently dried and visualized using an FEI 200 kV Sphera microscope.

Membrane Protein Characterization. MΦ-NPs were purified from free vesicles, membrane fragments, and unbound proteins by centrifugation at 16,000 × *g*. Macrophage cell lysates, membrane vesicles, and MΦ-NPs were mixed with lithium dodecyl sulfate (LDS) loading buffer to the same total protein concentration of 1 mg/mL as determined with a Pierce BCA assay (Life Technologies). Electrophoresis was carried out with NuPAGE Novex 4–12% Bis-Tris 10-well minigels in Mops running buffer with an XCell SureLock Electrophoresis System (Invitrogen). Western blot analysis was performed by using primary antibodies including rat anti-mouse CD14, rat anti-mouse CD126, rat anti-mouse CD130, rat anti-mouse CD284, Armenian hamster anti-mouse CD120a, Armenian hamster anti-mouse CD120b, and Armenian hamster anti-mouse CD119 (BioLegend). Corresponding IgG-horseradish peroxidase (HRP) conjugates were used for the secondary staining. Films were developed with ECL Western blotting substrate (Pierce) on a Mini-Medical/90 Developer (ImageWorks).

LPS and Cytokines Binding Studies. To study whether LPS binding with MΦ-NPs was dependent on LBP, CD14, or TLR4, the mixture of MΦ-NPs (1 mg/mL) and FITC-LPS (from *E. coli* O111:B4, 125 ng/mL; Sigma) in 1× PBS was added with FBS (10% as the source of LBP), anti-CD14 (10 μg/mL; BioLegend), or anti-TLR4 (10 μg/mL; Invivogen), respectively. The solution was incubated at 37 °C for 30 min. Following the incubation, MΦ-NPs were spun down with ultracentrifugation (16,000 × *g*). The fluorescence intensity from FITC-LPS remaining in the supernatant was measured. The fluorescence intensity from a FITC-LPS solution of 125 ng/mL served as 100%. The mixtures without adding FBS or antibodies were used as the controls. An equivalent amount of MΦ ghost (protein mass) was used as a control to assess the loss of membrane function during coating. The mixture added with nonspecific IgG from human serum was also included as a negative control to exclude the effect of the nonbinding domains of the antibody that may contribute to LPS inhibition. All experiments were performed in triplicate.

To quantify LPS removal with MΦ-NPs, MΦ-NPs (0.4 mg, 4 mg/mL) were mixed with LPS from *E. coli* K12 (Invivogen) with varying amount of 5, 10, 25, and 50 ng (50, 100, 250, and 500 ng/mL), respectively, in 1× PBS containing 10% FBS. In a parallel experiment, the removal was studied by fixing LPS amount at 50 ng (250 ng/mL) but varying the amount of MΦ-NPs at 0.1, 0.2, 0.3, and 0.4 mg (0.5, 1, 1.5, and 2 mg/mL), respectively. In both cases, the mixtures were incubated for 30 min and then spun down at 16,000 × *g* for 15 min to pellet the nanoparticles. The free LPS content in the supernatant was quantified by using limulus amebocyte lysate (LAL) assay (Thermo Fisher Scientific) per manufacturer's instructions. All experiments were performed in triplicate.

To determine MΦ-NP binding with cytokines, including IL-6, TNF-α, and IFN-γ, 100 μL of MΦ-NP samples (1 and 4 mg/mL) mixed with IL-6 (2,000 pg/mL), TNF-α (370 pg/mL), or IFN-γ (880 pg/mL) in PBS containing 10% FBS were incubated at 37 °C for 30 min. Following the incubation, the samples were centrifuged at 16,000 × *g* for 15 min to pellet the nanoparticles. Cytokine concentrations in the supernatant were quantified by using ELISA (BioLegend). All experiments were performed in triplicate.

LPS Neutralization in Vitro. Murine TLR4 reporter cells (HEK-Blue mTLR4 cells, Invivogen) were first used to determine LPS neutralization by MΦ-NPs. Cells were cultured in DMEM supplemented with 10% FBS, 1% pen–strep, 100 μg/mL normocin, 2 mM L-glutamine, and 1× HEK-Blue selection (Invivogen). In the study, 2.5×10^4 cells were seeded in each well of a 96-well plate with 160 μL HEK-Blue detection medium, followed by adding 20 μL of 100 ng/mL LPS in PBS. Then 20 μL of nanoparticle solution of MΦ-NPs, RBC-NPs, or PEG-NPs (all at a concentration of 10 mg/mL), was added into each well. Control wells were added with 20 μL PBS. Cells without any treatment served as the background. The mixture was incubated for 12 h. SEAP was quantified by measuring the absorbance at 630 nm with an Infinite M200 multiplate reader (Tecan). All experiments were performed in triplicate.

Production of iNO was also used to evaluate LPS neutralization with MΦ-NPs. Briefly, 2×10^4 J774 cells were seeded in each well of a 96-well plate. The cells were incubated with 10 μM of 2′, 7′-dichlorofluorescin-diacetate (DCFH-DA) (Sigma) in culture medium for 1 h and then washed three times with the culture medium. Then the wells were added with 180 μL of medium containing 10 ng/mL of LPS. Then 20 μL of nanoparticle solution of MΦ-NPs, RBC-NPs, or PEG-NPs (all at a concentration of 10 mg/mL), was added into each well. Twenty microliters of PBS was added to control wells. Cells without any treatment served as the background. The plate was incubated at 37 °C for 5 h. The production of iNO was quantified by measuring the fluorescence intensity at 520 nm using an excitation wavelength of 485 nm (Infinite M200 multiplate reader, Tecan). All experiments were performed in triplicate.

LPS neutralization with MΦ-NPs was further evaluated by examining E-selectin expression on HUVECs. Specifically, HUVECs were cultured to confluence in a 96-well plate. Then 200 μL of LPS (250 ng/mL) mixed with MΦ-NPs, RBC-NPs, or PEG-NPs (4 mg/mL) in culture medium was added to the cells and the plate was incubated at 37 °C. Cells added with LPS and PBS were used as controls. Three wells were used per sample. After 1, 2, 3, and 4 h of incubation at 37 °C, medium was removed and cells were washed with PBS. Then the cells were fixed with 4% paraformaldehyde (Sigma) at room temperature for 15 min. Following the fixation, cells were washed twice with PBS and blocked with 1% BSA (Sigma). Subsequently, the reagent was decanted and 50 μL of primary antibody (mouse anti-human E-selectin, 1:10 dilution in 1% BSA;

BioLegend) was added to each well and incubated at 37 °C for 45 min. Wells were then rinsed three times with 1× PBS before the addition of 50 μL of secondary antibody (HRP-conjugated anti-mouse IgG, 1:10 dilution in 1% BSA; BioLegend) followed by an incubation for 45 min at 37 °C. After this, wells were again rinsed three times with 1× PBS and after the final rinse, 100 μL of 3,3′,5,5′-tetramethylbenzidine (TMB) substrate solution was added to each well. The plate was incubated at 37 °C followed by measuring the absorbance at 450 nm.

To visually examine E-selectin expression, cells following the same treatment as the above experiment were incubated at 37 °C for 4 h and rinsed twice with PBS, fixed with 4% paraformaldehyde for 15 min, permeabilized in 0.2% Triton X-100 (Sigma) in buffer for 10 min, and then incubated with 1% BSA in PBS for 30 min. Cells were then stained with mouse anti-human E-selectin for 1 h, washed three times with 1× PBS, and then incubated with anti-mouse IgG Alexa 488 conjugates in 1% BSA in PBS for 1 h. Cell nuclei were stained with DAPI (1 mg/mL stock solution; Thermo Fisher Scientific). Fluorescence images were taken with an EVOS fluorescence microscope (Thermo Fisher Scientific).

Animal Care and Injections. All animal studies were approved under the guidelines of the University of California San Diego (UCSD) Institutional Animal Care and Use Committee. Mice were housed in an animal facility at UCSD under federal, state, local, and NIH guidelines for animal care. In the study, no inflammation was observed at the sites of injection.

Pharmacokinetics and Biodistribution Studies. The experiments were performed on 6-wk-old male ICR mice (Harlan Laboratories). To determine the circulation half-life, 150 μL of DiD-labeled MΦ-NPs (3 mg/mL) was injected i.v. through the tail vein. At 1, 15, and 30 min, and 1, 2, 4, 8, 24, 48, and 72 h postinjection, one drop of blood (~30 μL) was collected from each mouse via submandibular puncture with heparin-coated tubes. Then 20 μL of blood was mixed with 180 μL PBS in a 96-well plate for fluorescence measurement. Pharmacokinetic parameters were calculated to fit a two-compartment model. For biodistribution study, 150 μL of DiD-labeled MΦ-NPs (3 mg/mL) was injected i.v. through the tail vein. At 24, 48, and 72 h postinjection, organs including the liver, kidneys, spleen, brain, lungs, heart, and blood were collected from six randomly selected mice. The collected organs were weighed and then homogenized in PBS for fluorescence measurement. All fluorescence measurements were carried out with an Infinite M200 multiplate reader (Tecan).

LPS Neutralization in Vivo. The efficacy of MΦ-NPs in neutralizing LPS was first evaluated with a mouse endotoxemia model with 6-wk-old male BALB/c mice (Harlan). To evaluate the efficacy through cytokine production, mice were injected with 5 μg/kg LPS through the tail vein. After 15 min, MΦ-NPs, RBC-NPs, or PEG-NPs were injected at 200 mg/kg. Following the injections, blood samples (<30 μL) were collected at predetermined time points via submandibular puncture. Untreated mice and mice injected with LPS alone were used as controls. Cytokines, including IL-6 and TNF-α, in the plasma were quantified by ELISA as described above. In each group, six mice were used. To evaluate efficacy through survival, mice were first sensitized with D-galactosamine hydrochloride (Sigma-Aldrich) via i.p. injection at a dosage of 800 mg/kg. After 30 min of sensitization, LPS and nanoparticles were injected intravenously. Ten mice were used in each group.

LPS neutralization efficacy was also evaluated with a mouse bacteremia model. Specifically, 6-wk-old female C57BL/6 (The Jackson Laboratory) mice were injected intraperitoneally with 1×10^7 cfu of uropathogenic *E. coli* (UPEC) CFT073 suspended in 100 μL of 1× PBS. After 30 min, mice were randomly placed into two groups ($n = 10$), and each mouse was injected with 500 μL of MΦ-NPs at a concentration of 10 mg/mL in 10% sucrose solution intraperitoneally. Mice were killed 4 h after the injection. Blood and organs were collected and homogenized with a Mini Beadbeater-16 (BioSpec) in 1 mL of PBS. Proinflammatory cytokines in the blood, including IL-6, TNF-α, and IFN-γ, were quantified by a cytometric bead array per manufacturer's instructions (BD Biosciences). For bacterial enumeration, homogenized samples were serially diluted with PBS (from 10- to 10^7-fold) and plated onto agar plates. After 24 h of culture, bacterial colonies were counted. To evaluate efficacy through survival, the same experimental procedure was carried out and survival was monitored over a period of 60 h ($n = 10$).

ACKNOWLEDGMENTS. This work is supported by the National Science Foundation Grant DMR-1505699 (to L.Z.), the Defense Threat Reduction Agency Joint Science and Technology Office for Chemical and Biological Defense under Grant HDTRA1-14-1-0064 (to L.Z.), and NIH Grant 1R01HL125352 (to V.N.).

1. Angus DC, van der Poll T (2013) Severe sepsis and septic shock. *N Engl J Med* 369:840–851.
2. Cohen J (2002) The immunopathogenesis of sepsis. *Nature* 420:885–891.
3. Rittirsch D, Flierl MA, Ward PA (2008) Harmful molecular mechanisms in sepsis. *Nat Rev Immunol* 8:776–787.
4. Ranieri VM, et al.; PROWESS-SHOCK Study Group (2012) Drotrecogin alfa (activated) in adults with septic shock. *N Engl J Med* 366:2055–2064.
5. Gaieski DF, Edwards JM, Kallan MJ, Carr BG (2013) Benchmarking the incidence and mortality of severe sepsis in the United States. *Crit Care Med* 41:1167–1174.
6. Yaroustovsky M, et al. (2013) Prognostic value of endotoxin activity assay in patients with severe sepsis after cardiac surgery. *J Inflamm (Lond)* 10:8.
7. Grandel U, Grimminger F (2003) Endothelial responses to bacterial toxins in sepsis. *Crit Rev Immunol* 23:267–299.
8. Peters K, Unger RE, Brunner J, Kirkpatrick CJ (2003) Molecular basis of endothelial dysfunction in sepsis. *Cardiovasc Res* 60:49–57.
9. Wang Y (2014) Attenuation of berberine on lipopolysaccharide-induced inflammatory and apoptosis responses in beta-cells via TLR4-independent JNK/NF-κB path. *Pharm Biol* 52:532–538.
10. Nishio K, et al. (2013) Attenuation of lipopolysaccharide (LPS)-induced cytotoxicity by tocopherols and tocotrienols. *Redox Biol* 1:97–103.
11. Brandenburg K, Wiese A (2004) Endotoxins: Relationships between structure, function, and activity. *Curr Top Med Chem* 4:1127–1146.
12. Gabrielli L, et al. (2012) Recent approaches to novel antibacterials designed after LPS structure and biochemistry. *Curr Drug Targets* 13:1458–1471.
13. Kelesidis T, Falagas ME (2015) The safety of polymyxin antibiotics. *Expert Opin Drug Saf* 14:1687–1701.
14. Justo JA, Bosso JA (2015) Adverse reactions associated with systemic polymyxin therapy. *Pharmacotherapy* 35:28–33.
15. Cavaillon JM (2011) Polymyxin B for endotoxin removal in sepsis. *Lancet Infect Dis* 11: 426–427.
16. Fujii T, et al. (2016) Polymyxin B-immobilised haemoperfusion and mortality in critically ill patients with sepsis/septic shock: A protocol for a systematic review and meta-analysis. *BMJ Open* 6:e012908.
17. Raghavan R (2012) When access to chronic dialysis is limited: One center's approach to emergent hemodialysis. *Semin Dial* 25:267–271.
18. Zhang L, Leroux JC (2015) Current and forthcoming approaches for systemic detoxification. *Adv Drug Deliv Rev* 90:1–2.
19. Hu CMJ, et al. (2015) Nanoparticle biointerfacing by platelet membrane cloaking. *Nature* 526:118–121.
20. Hu CMJ, Fang RH, Copp J, Luk BT, Zhang L (2013) A biomimetic nanosponge that absorbs pore-forming toxins. *Nat Nanotechnol* 8:336–340.
21. Escajadillo T, Olson J, Luk BT, Zhang L, Nizet V (2017) A red blood cell membrane-camouflaged nanoparticle counteracts *Streptolysin O*-mediated virulence phenotypes of invasive group a streptococcus. *Front Pharmacol* 8:477.
22. Copp JA, et al. (2014) Clearance of pathological antibodies using biomimetic nanoparticles. *Proc Natl Acad Sci USA* 111:13481–13486.
23. Pang Z, et al. (2015) Detoxification of organophosphate poisoning using nanoparticle bioscavengers. *ACS Nano* 9:6450–6458.
24. Akira S, Takeda K, Kaisho T (2001) Toll-like receptors: Critical proteins linking innate and acquired immunity. *Nat Immunol* 2:675–680.
25. Medzhitov R (2001) Toll-like receptors and innate immunity. *Nat Rev Immunol* 1:135–145.
26. Schütt C (1999) Fighting infection: The role of lipopolysaccharide binding proteins CD14 and LBP. *Pathobiology* 67:227–229.
27. Triantafilou M, Triantafilou K (2002) Lipopolysaccharide recognition: CD14, TLRs and the LPS-activation cluster. *Trends Immunol* 23:301–304.
28. Zanoni I, et al. (2011) CD14 controls the LPS-induced endocytosis of toll-like receptor 4. *Cell* 147:868–880.
29. Schilling JD, Machkovech HM, He L, Diwan A, Schaffer JE (2013) TLR4 activation under lipotoxic conditions leads to synergistic macrophage cell death through a TRIF-dependent pathway. *J Immunol* 190:1285–1296.
30. Hagar JA, Powell DA, Aachoui Y, Ernst RK, Miao EA (2013) Cytoplasmic LPS activates caspase-11: Implications in TLR4-independent endotoxic shock. *Science* 341:1250–1253.
31. Martinon F, Chen X, Lee A-H, Glimcher LH (2010) TLR activation of the transcription factor XBP1 regulates innate immune responses in macrophages. *Nat Immunol* 11:411–418.
32. Spence S, et al. (2015) Targeting Siglecs with a sialic acid-decorated nanoparticle abrogates inflammation. *Sci Transl Med* 7:303ra140.
33. Gratton SEA, et al. (2007) Nanofabricated particles for engineered drug therapies: A preliminary biodistribution study of PRINT nanoparticles. *J Control Release* 121:10–18.
34. Hu C-MJ, et al. (2011) Erythrocyte membrane-camouflaged polymeric nanoparticles as a biomimetic delivery platform. *Proc Natl Acad Sci USA* 108:10980–10985.
35. Unger RE, Peters K, Sartoris A, Freese C, Kirkpatrick CJ (2014) Human endothelial cell-based assay for endotoxin as sensitive as the conventional limulus amebocyte lysate assay. *Biomaterials* 35:3180–3187.
36. Roger T, et al. (2009) Protection from lethal gram-negative bacterial sepsis by targeting toll-like receptor 4. *Proc Natl Acad Sci USA* 106:2348–2352.
37. Kang JH, et al. (2014) An extracorporeal blood-cleansing device for sepsis therapy. *Nat Med* 20:1211–1216.
38. Fang RH, et al. (2013) Lipid-insertion enables targeting functionalization of erythrocyte membrane-cloaked nanoparticles. *Nanoscale* 5:8884–8888.
39. Dehaini D, et al. (2017) Erythrocyte-platelet hybrid membrane coating for enhanced nanoparticle functionalization. *Adv Mater* 29:1606209.
40. Fang RH, et al. (2014) Cancer cell membrane-coated nanoparticles for anticancer vaccination and drug delivery. *Nano Lett* 14:2181–2188.